Shot noise of spin-polarized charge currents as a probe of spin coherence in spin-orbit coupled nanostructures

Ralitsa L. Dragomirova and Branislav K. Nikolić
Department of Physics and Astronomy, University of Delaware, Newark, Delaware 19716-2570, USA
(Received 16 November 2006; published 28 February 2007)

We generalize the scattering theory of quantum shot noise to include the full spin-density matrix of electrons injected from a spin filtering or ferromagnetic electrode into a quantum-coherent nanostructure governed by arbitrary spin-dependent interactions. This formalism yields the spin-resolved shot noise power for different experimental measurement setups—with ferromagnetic source and ferromagnetic or normal drain electrodes—whose evaluation for the diffusive multichannel quantum wires with the Rashba spin-orbit (SO) coupling shows how spin decoherence and dephasing lead to substantial enhancement of charge current fluctuations (characterized by Fano factors $>1/3$). However, these processes and the corresponding shot-noise increase are suppressed in narrow wires, so that charge transport experiments measuring the Fano factor $F_{\uparrow\rightarrow\uparrow\downarrow}$ in a ferromagnet/SO-coupled-wire/paramagnet setup also quantify the degree of phase coherence of transported spin—we predict a one-to-one correspondence between the magnitude of the spin-polarization vector and $F_{\uparrow\rightarrow\uparrow\downarrow}$.

DOI: 10.1103/PhysRevB.75.085328 PACS number(s): 73.23.−b, 72.70.+m, 72.25.−b, 71.70.Ej

I. INTRODUCTION

Over the past two decades, the exploration of the shot noise accompanying charge flow through mesoscopic conductors has become a major tool for gathering information about microscopic mechanisms of transport and correlations between charges which cannot be extracted from traditional conductance measurements.[1] Such nonequilibrium time-dependent fluctuations arise due to discreetness of charge, persist down to zero temperature (in contrast to thermal fluctuations which vanish at $T=0$), and require stochasticity induced by either quantum-mechanical[2] backscattering of charge carriers within a mesoscopic (i.e., smaller than the inelastic scattering length[3]) conductor or by random injection process (as in the textbook example of Schottky vacuum diode).

The zero-frequency shot-noise power $S=2FI$ of conventional unpolarized charge current with average value I in two-terminal noninteracting conductors reaches its maximum (the Poisson limit) characterized by the Fano factor $F=1$ when transport is determined by uncorrelated stochastic processes. On the other hand, the Pauli exclusion principle correlates electron motion and suppresses the shot noise $F<1$ of noninteracting carriers, while electron-electron interactions can also lead to super-Poissonian $F>1$ noise signatures.[4] For example, the well-known[5] and experimentally confirmed[3] $F=1/3$ universal suppression factor for noninteracting quasiparticles in two-terminal diffusive conductors is determined by the interplay of randomness in quantum-mechanical impurity scattering and the Pauli blocking imposed by their Fermi statistics.

In contrast to the wealth of information acquired on the shot noise in spin-degenerate transport, it is only recently that the study of *spin-dependent shot noise* in ferromagnet-normal systems[6] has been initiated in two-terminal[7–9] and multiterminal structures.[10–12] In such devices, ferromagnetic sources inject spin-polarized charge current into a paramagnetic region with interactions which affect the spin of transported electrons. For example, it has been shown that spin-flip scattering can substantially increase the shot noise above $F=1/3$ in diffusive wires attached to two ferromagnetic electrodes with antiparallel orientation of their magnetization,[7] as well as in the setup with the ferromagnetic source and normal drain (collecting both spin species) electrodes.[8] Thus, the enhanced shot-noise power reveals additional sources of current fluctuation when spin degeneracy is lifted and particles from spin-$\uparrow$ electron subsystem are converted into spin-$\downarrow$ electrons. The nonconservation of particles in each spin subsystem as a source of additional noise is quite analogous to a more familiar example of fluctuations of electromagnetic radiation in random optical media due to nonconservation of the number of photons.[13] Microscopically, spin flips are either instantaneous events generated by the collision of electrons with magnetic impurities and SO dependent scattering off static disorder[9] or continuous spin precession[8] during electron free propagation in magnetic fields imposed either externally or induced by intrinsic SO couplings[14] [whose "internal" magnetic field $\mathbf{B}_{\mathrm{int}}(\mathbf{p})$ is momentum dependent and spin splits the energy bands].

In particular, the crucial role played by the SO interactions in all-electrical control of spin in semiconductor nanostructures[15] has also ignited recent studies of their signatures on the shot noise.[12] It has been shown that the Rashba SO coupling in a two-dimensional electron gas (2DEG) can modulate the Fano factor of the shot noise of unpolarized charge current in clean beam splitter devices.[12] Moreover, the Rashba SO interaction is solely responsible for the nonzero noise[16] in ballistic chaotic dots where it introduces quantum effects into the regime where electrons otherwise follow deterministic classical trajectories (characterized[2] by $F=0$).

Despite these advances, key questions for the understanding of shot noise in SO-coupled nanostructures remain unanswered: *What is the connection between the Fano factor and the degree of quantum coherence* $|\mathbf{P}_{\mathrm{detect}}|$ *of transported spins? How does the shot noise depend on the spin-*

 ©2007 The American Physical Society

polarization vector $\mathbf{P}_{\text{inject}}$ *of injected spins and its direction with respect to* $\mathbf{B}_{\text{int}}(\mathbf{p})$? The spin-polarization vector of the detected current[17] $\mathbf{P}_{\text{detect}}$ is rotated by coherent precession, as well as shrunk $0 \leqslant |\mathbf{P}_{\text{detect}}| < 1$ by the D'yakonov-Perel' (DP) spin dephasing[15,18] due to random changes in $\mathbf{B}_{\text{int}}(\mathbf{p})$ after electron scatters off impurities or boundaries (note that these collisions themselves do not involve spin flip). Such different aspects of spin dynamics could leave distinctive signatures on the shot noise.[8]

At low temperatures, where small enough ($\lesssim 1$ μm) conductors become phase coherent and the Pauli blocking renders regular injection and collection of charge carriers from the bulk electrodes, the scattering theory of quantum transport provides[1,19] the celebrated formula for the shot-noise power in terms of the transmission eigenvalues T_n,

$$S = \frac{4e^3V}{h}\sum_{n=1}^{M} T_n(1-T_n). \tag{1}$$

Here, V is the linear response time-independent bias voltage.[1] The physical interpretation of Eq. (1) is quite transparent—in the basis of eigenchannels, which diagonalize $\mathbf{tt}^\dagger$ where $\mathbf{t}$ is the Landauer-Büttiker transmission matrix, a mesoscopic structure can be viewed as a parallel circuit of M (=number of transverse propagating orbital wave functions in the leads) independent one-dimensional conductors, each characterized by the transmission probability T_n. To get the shot noise through disordered systems, Eq. (1) has to be averaged[1] over a proper distribution of T_n. However, this standard route *becomes inapplicable* for spin-polarized injection where one has to take into account the *spin-density matrix* of injected electrons[17] and, therefore, perform the calculations in the *natural basis*[1] composed of spin-polarized conducting channels of the electrodes.[8]

Here, we address questions posed above by (i) deriving in Sec. II a generalization of the scattering-matrix-based formulas for the shot noise to include both the "direction" of injected spins and the degree of their quantum coherence, as encoded into the spin-polarization vector $\mathbf{P}_{\text{inject}}$ which determines their spin-density matrix $\hat{\rho}_{\text{inject}}=(\mathbf{1}+\mathbf{P}_{\text{inject}}\cdot\hat{\boldsymbol{\sigma}})/2$; and (ii) explicitly connecting in Sec. IV the value of the Fano factor in the right electrode to the degree of quantum coherence of phase-coherently transported spins $|\mathbf{P}_{\text{detect}}|$ extracted from a recently developed[17] scattering approach to their spin-density matrix $\hat{\rho}_{\text{detect}}=(\mathbf{1}+\mathbf{P}_{\text{detect}}\cdot\hat{\boldsymbol{\sigma}})/2$. We recall[20] that the density matrix $\hat{\rho}$ ($\hat{\rho}=\hat{\rho}^\dagger$, $\text{Tr}_{\text{spin}}\,\hat{\rho}=1$) of spin-$\frac{1}{2}$ particles is a 2×2 matrix ($\mathbf{1}$ denotes the 2×2 unit matrix),

$$\hat{\rho} = \begin{pmatrix} \rho_{\uparrow\uparrow} & \rho_{\uparrow\downarrow} \\ \rho_{\downarrow\uparrow} & \rho_{\downarrow\downarrow} \end{pmatrix} = \frac{1}{2}(\mathbf{1}+\mathbf{P}\cdot\hat{\boldsymbol{\sigma}}), \tag{2}$$

determined solely by measuring the three real numbers comprising the spin-polarization vector $\mathbf{P}=\text{Tr}[\hat{\rho}\hat{\boldsymbol{\sigma}}]$ as the expectation value of the spin operator $\hbar\mathbf{P}/2=\langle\hbar\hat{\boldsymbol{\sigma}}/2\rangle$. The magnitude $|\mathbf{P}|$ quantifies the degree of quantum coherence. Thus, $\hat{\rho}$ and the corresponding $\mathbf{P}$ provide the most general quantum-mechanical description of a spin-$\frac{1}{2}$ system, accounting for both pure (i.e., fully coherent) $\hat{\rho}^2=\hat{\rho}\Leftrightarrow|\mathbf{P}|=1$ and mixed $\hat{\rho}^2\neq\hat{\rho}\Leftrightarrow 0\leqslant|\mathbf{P}|<1$ states. Our spin-dependent shot-noise formalism is applied to Rashba SO-coupled quantum wires of different widths (where transverse confinement affects the degree of transported spin coherence[21]) in Sec. III, and its principal results are contrasted with related spin-dependent shot-noise studies in two-terminal setups in Sec. V. We conclude in Sec. VI.

II. SCATTERING APPROACH TO SPIN-DEPENDENT SHOT NOISE

The analysis of the spin-dependent shot noise requires the evaluation of correlations between spin-resolved charge currents $I^\uparrow$ and $I^\downarrow$ due to the flow of spin-$\uparrow$ and spin-$\downarrow$ electrons through the terminals of a nanostructure,[22]

$$S_{\alpha\beta}^{\sigma\sigma'}(t-t') = \frac{1}{2}\langle\delta\hat{I}_\alpha^\sigma(t)\,\delta\hat{I}_\beta^{\sigma'}(t') + \delta\hat{I}_\beta^{\sigma'}(t')\,\delta\hat{I}_\alpha^\sigma(t)\rangle. \tag{3}$$

Here, $\hat{I}_\alpha^\sigma(t)$ is the quantum-mechanical operator of the spin-resolved ($\sigma=\uparrow,\downarrow$) charge current in lead α. The current-fluctuation operator at time t in lead α is $\delta\hat{I}_\alpha(t)=\hat{I}_\alpha(t)-\langle\hat{I}_\alpha(t)\rangle$. We use $\langle\cdots\rangle$ to denote both quantum-mechanical and statistical averaging over the states in the macroscopic reservoirs to which a mesoscopic conductor is attached via semi-infinite interaction-free leads. The spin-resolved noise power between terminals α and β is (conventionally defined[1] as twice) the Fourier transform of Eq. (3),

$$S_{\alpha\beta}^{\sigma\sigma'}(\omega) = 2\int d(t-t')e^{-i\omega(t-t')}S_{\alpha\beta}^{\sigma\sigma'}(t-t'). \tag{4}$$

The noise power of the total charge current $I_\alpha=I_\alpha^\uparrow+I_\alpha^\downarrow$ is then given by

$$S_{\alpha\beta}(\omega) = S_{\alpha\beta}^{\uparrow\uparrow}(\omega) + S_{\alpha\beta}^{\downarrow\downarrow}(\omega) + S_{\alpha\beta}^{\uparrow\downarrow}(\omega) + S_{\alpha\beta}^{\downarrow\uparrow}(\omega). \tag{5}$$

The scattering theory of quantum transport gives for the operator of *spin-resolved* charge current of spin-σ electrons flowing through terminal α

$$\hat{I}_\alpha^\sigma(t) = \frac{e}{h}\sum_{n=1}^{M}\int\int dE dE'\, e^{i(E-E')t/\hbar}[\hat{a}_{\alpha n}^{\sigma\dagger}(E)\hat{a}_{\alpha n}^{\sigma}(E') - \hat{b}_{\alpha n}^{\sigma\dagger}(E)\hat{b}_{\alpha n}^{\sigma}(E')]. \tag{6}$$

The operator $\hat{a}_{\alpha n}^{\sigma\dagger}(E)$ [$\hat{a}_{\alpha n}^{\sigma}(E)$] creates [annihilates] incoming electrons in lead α, which have energy E and spin σ and the orbital part of their wave function is the transverse propagating mode $|n\rangle$. Similarly, $\hat{b}_{\alpha n}^{\sigma\dagger}$, $\hat{b}_{\alpha n}^{\sigma}$ denote spin-σ electrons in the outgoing states. Using this expression in Eq. (3) and taking its Fourier transform leads to the following formula for the spin-resolved noise power spectrum:

$$S_{\alpha\beta}^{\sigma\sigma'}(\omega) = \frac{e^2}{h}\int dE \sum_{\gamma,\gamma'}\sum_{\rho,\rho'=\uparrow,\downarrow}\text{Tr}[\mathbf{A}_{\gamma\gamma'}^{\rho\rho'}(\alpha,\sigma,E,E+\hbar\omega) \times \mathbf{A}_{\gamma'\gamma}^{\rho'\rho}(\beta,\sigma',E+\hbar\omega,E)]\{f_\gamma^\rho(E)[1-f_{\gamma'}^{\rho'}(E+\hbar\omega)] + f_{\gamma'}^{\rho'}(E+\hbar\omega)[1-f_\gamma^\rho(E)]\}. \tag{7}$$

Here, $f_\gamma^\rho(E)$ is the Fermi function of spin-ρ electrons ($\rho=\uparrow,\downarrow$), kept at temperature T_γ and with spin-dependent chemical potential μ_γ^ρ in lead γ. The Büttiker current matrix[19] $\mathbf{A}_{\beta\gamma}^{\rho\rho'}(\alpha,\sigma,E,E')$, whose elements are

$$[\mathbf{A}_{\beta\gamma}^{\rho\rho'}(\alpha,\sigma,E,E')]_{mn} = \delta_{mn}\delta_{\beta\alpha}\delta_{\gamma\alpha}\delta^{\sigma\rho}\delta^{\sigma\rho'} - \sum_k [\mathbf{s}_{\alpha\beta}^{\sigma\rho\dagger}(E)]_{mk}[\mathbf{s}_{\alpha\gamma}^{\sigma\rho'}(E')]_{kn}, \tag{8}$$

is now generalized to explicitly include spin degrees of freedom through the spin-resolved scattering matrix connecting operators $\hat{a}_{\alpha n}^\sigma(E)$ and $\hat{b}_{\alpha n}^\sigma(E)$ via $\hat{b}_{\alpha n}^\sigma(E)=\Sigma_{\beta m}[\mathbf{s}_{\alpha\beta}^{\sigma\sigma'}]_{nm}(E)\hat{a}_{\beta m}^{\sigma'}(E)$. In the zero-temperature limit, the thermal (Johnson-Nyquist) contribution to the noise vanishes and the Fermi function becomes a step function, $f_\alpha^\rho(E)=\theta(E-\mu_\alpha^\rho)$. Evaluation of Eq. (7) for zero temperature and zero frequency, $S_{\alpha\beta}^{\sigma\sigma'}\equiv S_{\alpha\beta}^{\sigma\sigma'}$ ($\omega=0$, $T=0$), in the left lead $\alpha=2=\beta$ of a two-terminal mesoscopic device yields our principal result—the scattering theory formula for the shot noise arising in the course of propagation of spin-polarized current through a region with spin-dependent interactions:

$$S_{22}^{\uparrow\uparrow} = \frac{2e^2}{h}\Bigg[\mathrm{Tr}(\mathbf{t}_{21}^{\uparrow\uparrow}\mathbf{t}_{21}^{\uparrow\uparrow\dagger})eV + \mathrm{Tr}(\mathbf{t}_{21}^{\uparrow\downarrow}\mathbf{t}_{21}^{\uparrow\downarrow\dagger})\frac{1-|\mathbf{P}_{\mathrm{inject}}|}{1+|\mathbf{P}_{\mathrm{inject}}|}eV - \mathrm{Tr}(\mathbf{t}_{21}^{\uparrow\downarrow}\mathbf{t}_{21}^{\uparrow\downarrow\dagger}\mathbf{t}_{21}^{\uparrow\downarrow}\mathbf{t}_{21}^{\uparrow\downarrow\dagger})\frac{1-|\mathbf{P}_{\mathrm{inject}}|}{1+|\mathbf{P}_{\mathrm{inject}}|}eV - \mathrm{Tr}(\mathbf{t}_{21}^{\uparrow\uparrow}\mathbf{t}_{21}^{\uparrow\uparrow\dagger}\mathbf{t}_{21}^{\uparrow\uparrow}\mathbf{t}_{21}^{\uparrow\uparrow\dagger})eV - 2\,\mathrm{Tr}(\mathbf{t}_{21}^{\uparrow\downarrow}\mathbf{t}_{21}^{\uparrow\downarrow\dagger}\mathbf{t}_{21}^{\uparrow\uparrow}\mathbf{t}_{21}^{\uparrow\uparrow\dagger})\frac{1-|\mathbf{P}_{\mathrm{inject}}|}{1+|\mathbf{P}_{\mathrm{inject}}|}eV\Bigg], \tag{9a}$$

$$S_{22}^{\downarrow\downarrow} = \frac{2e^2}{h}\Bigg[\mathrm{Tr}(\mathbf{t}_{21}^{\downarrow\downarrow}\mathbf{t}_{21}^{\downarrow\downarrow\dagger})\frac{1-|\mathbf{P}_{\mathrm{inject}}|}{1+|\mathbf{P}_{\mathrm{inject}}|}eV + \mathrm{Tr}(\mathbf{t}_{21}^{\downarrow\uparrow}\mathbf{t}_{21}^{\downarrow\uparrow\dagger})eV - \mathrm{Tr}(\mathbf{t}_{21}^{\downarrow\downarrow}\mathbf{t}_{21}^{\downarrow\downarrow\dagger}\mathbf{t}_{21}^{\downarrow\downarrow}\mathbf{t}_{21}^{\downarrow\downarrow\dagger})\frac{1-|\mathbf{P}_{\mathrm{inject}}|}{1+|\mathbf{P}_{\mathrm{inject}}|}eV - \mathrm{Tr}(\mathbf{t}_{21}^{\downarrow\uparrow}\mathbf{t}_{21}^{\downarrow\uparrow\dagger}\mathbf{t}_{21}^{\downarrow\uparrow}\mathbf{t}_{21}^{\downarrow\uparrow\dagger})eV - 2\,\mathrm{Tr}(\mathbf{t}_{21}^{\downarrow\uparrow}\mathbf{t}_{21}^{\downarrow\uparrow\dagger}\mathbf{t}_{21}^{\downarrow\downarrow}\mathbf{t}_{21}^{\downarrow\downarrow\dagger})\frac{1-|\mathbf{P}_{\mathrm{inject}}|}{1+|\mathbf{P}_{\mathrm{inject}}|}eV\Bigg], \tag{9b}$$

$$S_{22}^{\uparrow\downarrow} = -\frac{2e^2}{h}\Bigg[\mathrm{Tr}(\mathbf{t}_{21}^{\downarrow\uparrow}\mathbf{t}_{21}^{\uparrow\uparrow\dagger}\mathbf{t}_{21}^{\uparrow\downarrow}\mathbf{t}_{21}^{\downarrow\downarrow\dagger})\frac{1-|\mathbf{P}_{\mathrm{inject}}|}{1+|\mathbf{P}_{\mathrm{inject}}|}eV + \mathrm{Tr}(\mathbf{t}_{21}^{\downarrow\uparrow}\mathbf{t}_{21}^{\uparrow\uparrow\dagger}\mathbf{t}_{21}^{\uparrow\uparrow}\mathbf{t}_{21}^{\downarrow\uparrow\dagger})eV + \mathrm{Tr}(\mathbf{t}_{21}^{\downarrow\downarrow}\mathbf{t}_{21}^{\downarrow\uparrow\dagger}\mathbf{t}_{21}^{\uparrow\uparrow}\mathbf{t}_{21}^{\downarrow\uparrow\dagger})\frac{1-|\mathbf{P}_{\mathrm{inject}}|}{1+|\mathbf{P}_{\mathrm{inject}}|}eV + \mathrm{Tr}(\mathbf{t}_{21}^{\downarrow\downarrow}\mathbf{t}_{21}^{\downarrow\uparrow\dagger}\mathbf{t}_{21}^{\uparrow\downarrow}\mathbf{t}_{21}^{\downarrow\downarrow\dagger})\frac{1-|\mathbf{P}_{\mathrm{inject}}|}{1+|\mathbf{P}_{\mathrm{inject}}|}eV\Bigg], \tag{9c}$$

$$S_{22}^{\downarrow\uparrow} = -\frac{2e^2}{h}\Bigg[\mathrm{Tr}(\mathbf{t}_{21}^{\uparrow\uparrow}\mathbf{t}_{21}^{\downarrow\uparrow\dagger}\mathbf{t}_{21}^{\downarrow\downarrow}\mathbf{t}_{21}^{\downarrow\uparrow\dagger})\frac{1-|\mathbf{P}_{\mathrm{inject}}|}{1+|\mathbf{P}_{\mathrm{inject}}|}eV + \mathrm{Tr}(\mathbf{t}_{21}^{\uparrow\uparrow}\mathbf{t}_{21}^{\downarrow\uparrow\dagger}\mathbf{t}_{21}^{\downarrow\uparrow}\mathbf{t}_{21}^{\uparrow\uparrow\dagger})eV + \mathrm{Tr}(\mathbf{t}_{21}^{\uparrow\downarrow}\mathbf{t}_{21}^{\downarrow\uparrow\dagger}\mathbf{t}_{21}^{\downarrow\downarrow}\mathbf{t}_{21}^{\uparrow\uparrow\dagger})\frac{1-|\mathbf{P}_{\mathrm{inject}}|}{1+|\mathbf{P}_{\mathrm{inject}}|}eV + \mathrm{Tr}(\mathbf{t}_{21}^{\uparrow\downarrow}\mathbf{t}_{21}^{\downarrow\downarrow\dagger}\mathbf{t}_{21}^{\downarrow\uparrow}\mathbf{t}_{21}^{\uparrow\uparrow\dagger})\frac{1-|\mathbf{P}_{\mathrm{inject}}|}{1+|\mathbf{P}_{\mathrm{inject}}|}eV\Bigg]. \tag{9d}$$

Here, the elements of the transmission matrix $\mathbf{t}_{21}^{\sigma\sigma'}$, which is a block of the full scattering matrix, determine the probability $|[\mathbf{t}_{21}^{\sigma\sigma'}]_{nm}|^2$ for spin-σ' electron incident in lead 1 in the orbital conducting channel $|m\rangle$ to be transmitted to lead 2 as spin-σ electron in channel $|n\rangle$. The direction of the spin-polarization vector of injected electrons selects the spin-quantization axis for $\uparrow$, $\downarrow$. Its magnitude quantifies the degree of spin polarization which was introduced[12] into Eq. (7) via the spin-dependent electrochemical potentials in the injecting (left) lead, $\mu_1^\uparrow=E_F+eV$ and $\mu_1^\downarrow=E_F+eV(1-|\mathbf{P}_{\mathrm{inject}}|)/(1+|\mathbf{P}_{\mathrm{detect}}|)$. In the collecting (right) lead, the electrochemical potentials for both spin species are the same, $\mu_2^\uparrow=\mu_2^\downarrow=E_F$, where E_F is the Fermi energy. For instance, injection of fully spin-$\uparrow$ polarized current $|\mathbf{P}_{\mathrm{inject}}|=1$ from the left lead (e.g., made of half-metallic ferromagnet) means that there is no voltage drop for spin-$\downarrow$ electrons, $\mu_1^\downarrow=\mu_2^\downarrow=E_F$, so that they do not contribute to transport.

Equations (9), together with the expressions for average spin-resolved currents collected in the right lead,

$$I_2^\uparrow \equiv \langle \hat{I}_2^\uparrow(t)\rangle = \left(G_{21}^{\uparrow\uparrow} + G_{21}^{\uparrow\downarrow}\frac{1-|\mathbf{P}_{\mathrm{inject}}|}{1+|\mathbf{P}_{\mathrm{inject}}|}\right)V, \tag{10a}$$

$$I_2^\downarrow \equiv \langle \hat{I}_2^\downarrow(t)\rangle = \left(G_{21}^{\downarrow\uparrow} + G_{21}^{\downarrow\downarrow}\frac{1-|\mathbf{P}_{\mathrm{inject}}|}{1+|\mathbf{P}_{\mathrm{inject}}|}\right)V, \tag{10b}$$

define the Fano factors for parallel and antiparallel spin-valve setups,

$$F_{\uparrow\to\uparrow} = \frac{S_{22}^{\uparrow\uparrow}(|\mathbf{P}_{\mathrm{inject}}|=1)}{2eI_2^\uparrow(|\mathbf{P}_{\mathrm{inject}}|=1)}, \tag{11}$$

$$F_{\uparrow\to\downarrow} = \frac{S_{22}^{\downarrow\downarrow}(|\mathbf{P}_{\mathrm{inject}}|=1)}{2eI_2^\downarrow(|\mathbf{P}_{\mathrm{inject}}|=1)}. \tag{12}$$

These equations also give us the Fano factor for a ferromagnet/SO-coupled-wire/paramagnet configuration,

$$F_{\uparrow\to\uparrow\downarrow} = \frac{S_{22}(|\mathbf{P}_{\mathrm{inject}}|=1)}{2eI_2(|\mathbf{P}_{\mathrm{inject}}|=1)}, \tag{13}$$

where $I_2=I_2^\uparrow+I_2^\downarrow$ is the sum of both spin-resolved currents collected in the right paramagnetic lead. Here, the spin-resolved two-terminal conductances are given by the Landauer-type formula

$$G_{21}^{\sigma\sigma'} = \frac{e^2}{h}\sum_{n,m=1}^{M}|[\mathbf{t}_{21}^{\sigma\sigma'}]_{nm}|^2. \tag{14}$$

The consequences of the scattering theory expressions, Eqs. (9) and (10), can be worked out either by analytical means (such as the random matrix theory,[8] applicable for[23] $L\ll L_{\mathrm{SO}}$, or matching of the wave functions across single-or at most two-channel structures[12]) or by numerically exact real⊗spin space Green's functions[17] employed here to take the microscopic Hamiltonian of both weakly ($L\ll L_{\mathrm{SO}}$) and strongly ($L\gtrsim L_{\mathrm{SO}}$) SO-coupled *multichannel* nanostructures

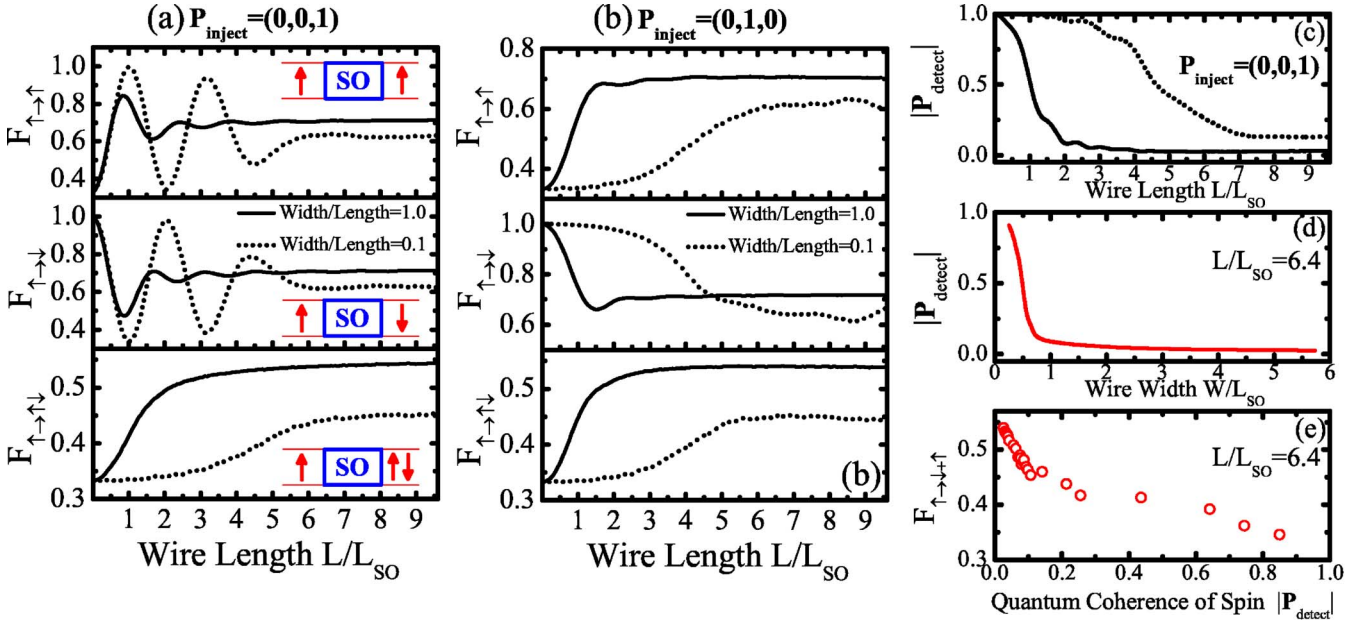

FIG. 1. (Color online) Panels (a) and (b) show the Fano factor vs the spin precession length L_{SO} for different two-terminal setups where 100% spin-↑ polarized charge current is injected from the source electrode (e.g., half-metallic ferromagnet) into a diffusive Rashba SO-coupled wire and spin-resolved charge currents $I^{\uparrow}$ (top), $I^{\downarrow}$ (middle), or both $I^{\uparrow}+I^{\downarrow}$ (bottom) are collected in the drain electrode. Panel (c) shows the corresponding decay of the degree of phase coherence of transported spin, as quantified by the magnitude of the spin-polarization vector of charge current which is $|\mathbf{P}_{\text{inject}}|=1$ (signifying fully coherent pure spin state) in the left lead and pointing along the z axis in (a) and the y axis in (b). For fixed L and L_{SO}, the decay of $|\mathbf{P}_{\text{detect}}|$ is suppressed in narrow wires [panel (d)], which establishes a one-to-one correspondence between the Fano factor $F_{\uparrow\to\uparrow\downarrow}$ and $|\mathbf{P}_{\text{detect}}|$ [panel (e)]. Note that the Fano factors attaining universal value[3,5] $F_{\uparrow\to\uparrow}=F_{\uparrow\to\uparrow\downarrow}=1/3$ in the limit of zero SO coupling $L/L_{SO}\to 0$ demonstrate that our wires are in the diffusive transport regime for selected disorder strengths.

as an input. Here, we introduce relevant length scales: the system size L and the spin precession length L_{SO}, on which spin precesses by an angle π (i.e., state $|\uparrow\rangle$ evolves into $|\downarrow\rangle$). The central quantity of this formalism is the retarded Green's function of the scattering region $\hat{G}^r=[E-\hat{H}_{\text{open}}]^{-1}$ associated with the Hamiltonian $\hat{H}_{\text{open}}=\hat{H}+\hat{\Sigma}_1^{r,\uparrow}+\hat{\Sigma}_1^{r,\downarrow}+\hat{\Sigma}_2^{r,\uparrow}+\hat{\Sigma}_2^{r,\downarrow}$ of the open system where (non-Hermitian) retarded self-energies $\hat{\Sigma}_{\alpha}^{r,\sigma}$ introduced by the interaction with the leads determine escape rates of spin-σ electrons into the electrodes. The block $\hat{G}_{21}^{r,\sigma\sigma'}$ of the retarded Green's function matrix, consisting of those matrix elements which connect the layer of the sample attached to lead 1 to the layer of the sample attached to lead 2, yields the spin-resolved transmission matrix through

$$\mathbf{t}_{21}^{\sigma\sigma'}=2\sqrt{-\operatorname{Im}\hat{\Sigma}_2^{r,\sigma}}\cdot\hat{G}_{21}^{r,\sigma\sigma'}\cdot\sqrt{-\operatorname{Im}\hat{\Sigma}_1^{r,\sigma'}}. \tag{15}$$

For simplicity, we assume that $\hat{\Sigma}^{r,\uparrow}=\hat{\Sigma}^{r,\downarrow}$, which experimentally corresponds to identical conditions for injection of both spin species.

III. SHOT NOISE IN DIFFUSIVE RASHBA SO-COUPLED WIRES

We focus on quantum wires realized using 2DEG with the Rashba SO coupling[14] induced by structural inversion asymmetry of the semiconductor heterostructure hosting the 2DEG in the xy plane. The wires are described by the effective mass Hamiltonian

$$\hat{H}=\frac{\hat{p}_x^2+\hat{p}_y^2}{2m^*}+\frac{\alpha}{\hbar}(\hat{p}_y\otimes\hat{\sigma}_x-\hat{p}_x\otimes\hat{\sigma}_y)+V_{\text{confinement}}(y)+V_{\text{disorder}}(x,y), \tag{16}$$

where $\hat{\boldsymbol{\sigma}}=(\hat{\sigma}_x,\hat{\sigma}_y,\hat{\sigma}_z)$ denotes the vector of the Pauli spin matrices. The internal magnetic field $\mathbf{B}_{\text{int}}(\mathbf{p})=-(2\alpha/g\mu_B)(\hat{\mathbf{p}}\times\hat{z})$ ($\hat{z}$ is the unit vector orthogonal to 2DEG) corresponding to the Rashba SO coupling is nearly parallel to the transverse y axis in the case of quantum wires.[17] Therefore, the injected z-axis polarized spins precess within the wires, while the y-axis polarized spins are in the eigenstates of the corresponding Zeeman term and do not precess.[17] This leads to a difference in the shot noise when changing the spin-polarization vector of the injected current in the "polarizer-analyzer" scheme in the top and middle panels of Figs. 1(a) and 1(b).

Moreover, in both cases and within the asymptotic limit $L\gg L_{SO}$ (L is the wire length), we find the shot-noise increase above the universal Fano factor $F=1/3$ for all three measurement geometries in Fig. 1:

(1) spin valves with parallel magnetization of the electrodes where ↑-electrons are injected from the left lead and ↑-electrons are collected in the right lead, a situation described by the Fano factor $F_{\uparrow\to\uparrow}$;

(2) spin valves with antiparallel magnetization of the electrodes where ↑-electrons are injected through a perfect Ohmic contact and ↓-electrons are collected, as described by the Fano factor $F_{\uparrow\to\downarrow}$; and

(3) a setup with only one spin-selective electrode where ↑-electrons are injected and both ↑- and ↓-electrons are collected in the normal drain electrode, as described by the Fano factor $F_{\uparrow\to\uparrow\downarrow}$.

The spin precession length defined by the clean Rashba Hamiltonian $L_{\mathrm{SO}}=\pi\hbar^2/(2m^*\alpha)$ also plays the role of a characteristic length scale for exponentially decaying spin polarization in the DP spin dephasing in weakly disordered *bulk* systems.[15,18,24] For very small SO coupling and, therefore, large $L_{\mathrm{SO}}\to\infty$, the Fano factors $F_{\uparrow\to\uparrow}$ and $F_{\uparrow\to\uparrow\downarrow}$ start from the universal value $F=1/3$ characterizing the diffusive unpolarized transport and then increase toward their asymptotic values, $F_{\uparrow\to\uparrow}(L\gg L_{\mathrm{SO}})\approx F_{\uparrow\to\downarrow}(L\gg L_{\mathrm{SO}})\simeq 0.7$ and $F_{\uparrow\to\uparrow\downarrow}(L\gg L_{\mathrm{SO}})\simeq 0.55$. Such enhancement of the spin-dependent shot noise is due to spin *decoherence* and *dephasing* processes[17] in SO-coupled structures that reduce the off-diagonal elements of the current spin-density matrix $\hat{\rho}_{\mathrm{detect}}$. Note that in these setups, the density matrix $\hat{\rho}^2_{\mathrm{inject}}=\hat{\rho}_{\mathrm{inject}}$ describes pure injected spin states from the left lead.

However, these asymptotic Fano factor values are lowered in narrow wires, where transverse confinement slows down the DP spin relaxation in the picture of semiclassical spin diffusion,[18] or reduces the size of the "environment" of orbital conducting channels (i.e., their number) to which the spin can entangle in fully quantum transport picture[17] employed to obtain $|\mathbf{P}_{\mathrm{detect}}|$ vs wire width W (at constant length L and the Rashba SO coupling strength) in Fig. 1(d). The geometrical confinement effects increasing spin coherence in narrow wires[17,18,24] have been confirmed in a very recent optical spin detection experiment.[21] They might be essential for the realization of all-electrical semiconductor spintronic devices,[15] where spin is envisaged to be manipulated via SO couplings while avoiding their detrimental dephasing effects.[17] Thus, Fig. 1(e) demonstrates an exciting possibility for an experimental tool to quantify phase coherence of transported spin via purely electrical means, where the measurement of the Fano factor $F_{\uparrow\to\uparrow\downarrow}$ does not require demanding spin-selective detection in the right lead.

The shot noise in the antiparallel configuration reaches the full Poissonian value $F_{\uparrow\to\downarrow}(L\ll L_{\mathrm{SO}})\simeq 1$ in the limit of small SO coupling, since the probability that the spin state which has huge overlap with $|\uparrow\rangle$ can enter into the right electrode with empty spin-↑ states is minuscule. This leads to a tunneling-type[1,7] shot noise where electrons propagate independently without being correlated by the Fermi statistics. In the asymptotic limit $L\gg L_{\mathrm{SO}}$, injected spins lose their memory on a very short length scale, so that $F_{\uparrow\to\downarrow}(L\gg L_{\mathrm{SO}})$ acquires the same asymptotic value as $F_{\uparrow\to\uparrow}(L\gg L_{\mathrm{SO}})$.

Since the present spintronic experiments are usually conducted by injecting partially spin-polarized charge currents $|\mathbf{P}_{\mathrm{inject}}|<1$, we employ our general formulas [Eq. (9)] to obtain the Fano factor,

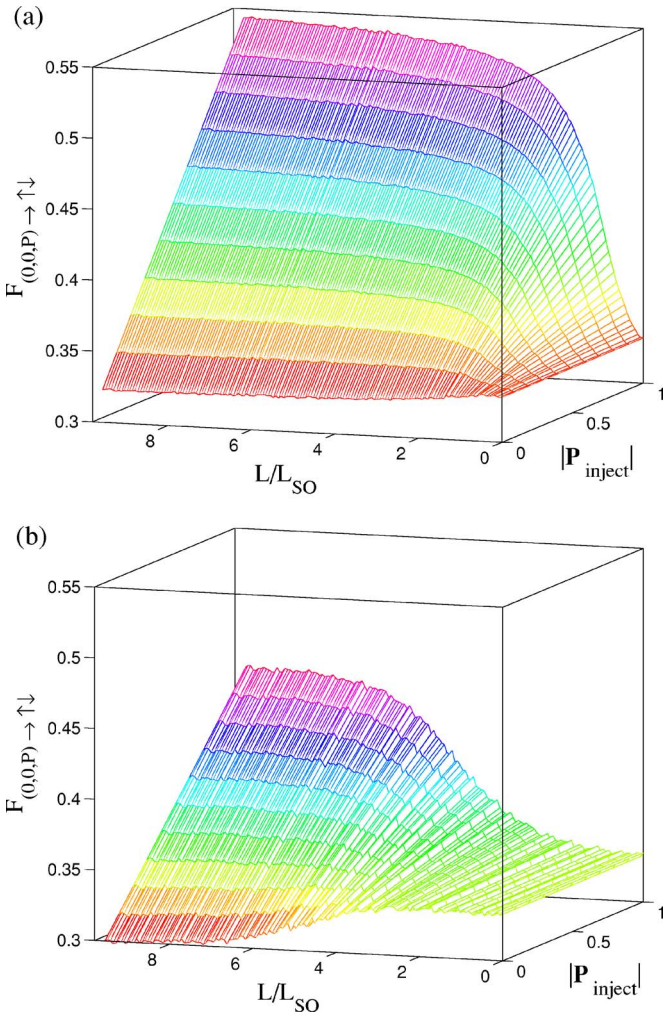

FIG. 2. (Color online) Fano factor as the function of SO coupling strength L/L_{SO} and $|\mathbf{P}_{\mathrm{inject}}|$ for a two-terminal measuring setup where partially spin-polarized current [comprised of electrons with spin-polarization vector $\mathbf{P}_{\mathrm{inject}}=(0,0,P)$] is injected from an ideal source lead into a diffusive Rashba SO-coupled wire and charge current of both spins $I^{\uparrow}+I^{\downarrow}$ is collected by the spin-nonselective drain lead. In panel (a), the wire length L and width W are the same $W/L=1$, while panel (b) plots $F_{(0,0,P)\to\uparrow\downarrow}$ in narrow wires, $W/L=0.1$. Note that the limiting curves extracted for $|\mathbf{P}_{\mathrm{inject}}|=1$ correspond to the bottom panel in Fig. 1(a).

$$F_{(0,0,P)\to\uparrow\downarrow}=\frac{S_{22}[\mathbf{P}_{\mathrm{inject}}=(0,0,P)]}{2eI_2[\mathbf{P}_{\mathrm{inject}}=(0,0,P)]}. \tag{17}$$

This represents a generalization of $F_{\uparrow\to\uparrow\downarrow}$ to characterize the shot noise in an experimental setup where partially polarized (along the z axis) electrons are injected from the left lead while both spin species are collected in the right lead. Figure 2 suggests that predictions for the excess shot noise $F_{(0,0,P)\to\uparrow\downarrow}>1/3$ should be observable even for small polarization of injected current $|\mathbf{P}_{\mathrm{inject}}|\equiv P\gtrsim 10\%$.

IV. FANO FACTOR AS QUANTIFIER OF TRANSPORTED SPIN COHERENCE

To understand the evolution of quantum coherence of transported spin, we use fully quantum transport formalism

of Ref. 17, which treats both the spin dynamics and orbital propagation of electrons to which the spins are attached phase coherently. This allows us to obtain the spin-density matrix of charge current in the right lead in terms of the same spin-resolved transmission matrix $\mathbf{t}_{21}^{\sigma\sigma'}$ which determines the shot-noise power $S_{22}^{\sigma\sigma'}$. Note that traditional description of DP spin dephasing treats charge propagation semiclassically, while the dynamics of its spin is described via quantum evolution of the spin-density matrix.[15,18]

Here, we briefly summarize principal steps, put forth by Nikolić and Souma in Ref. 17, which make it possible to define the spin-density matrix of an ensemble of phase-coherently transported spins comprising the detected current in the right lead within the framework of the scattering approach to quantum transport. Suppose that a spin-↑ polarized electron is injected from the left lead through a conducting channel $|\text{in}\rangle \equiv |m\rangle \otimes |\uparrow\rangle$. Then, a pure state emerging in the right lead after electron has traversed the sample is described by the linear combination of the outgoing channels, $|\text{out}\rangle = \Sigma_{n\sigma}[\mathbf{t}_{21}^{\sigma\uparrow}]_{nm}|n\rangle \otimes |\sigma\rangle$. Such *nonseparable* state encodes entanglement of spin and the environment composed of orbital conducting channels $|n\rangle$. Any entanglement to the environment is a source of *spin decoherence*,[25] since the spin-density matrix obtained by tracing the full density matrix $|\text{out}\rangle\langle\text{out}|$ of the pure state $|\text{out}\rangle$ over the orbital transverse propagating modes $|n\rangle$ in the right lead,

$$\hat{\rho}^{m\uparrow\to\text{out}} = \frac{1}{Z}\text{Tr}_{\text{orbital}}|\text{out}\rangle\langle\text{out}| = \frac{1}{Z}\sum_{n=1}^{M}\langle n|\text{out}\rangle\langle\text{out}|n\rangle, \tag{18}$$

will have, in general, the polarization vector $|\mathbf{P}^{m\uparrow\to\text{out}}| < 1$ when transport takes place through multichannel wires[17] (here, Z is the normalization factor ensuring that $\text{Tr}_{\text{spin}}\,\hat{\rho}^{m\uparrow\to\text{out}} = 1$).

Further decrease of the observable degree of quantum coherence encoded by the off-diagonal elements[25] of the spin-density matrix is generated by *spin dephasing*[17,26] due to averaging over all orbital incoming channels, $\hat{\rho}_{\text{detect}}^{\uparrow} = \Sigma_m \hat{\rho}^{m\uparrow\to\text{out}}$. Such dephasing remains relevant even if every electron in the right lead continues to be in the orbital conducting channel through which it was originally injected, so that $|\text{out}\rangle$ emerges in the right lead as a separable quantum state. This procedure finally leads to the spin-density matrix associated with the detected charge current in the right lead,[17]

$$\hat{\rho}_{\text{detect}}^{\uparrow} = \frac{e^2/h}{G_{21}^{\uparrow\uparrow} + G_{21}^{\downarrow\uparrow}}\sum_{n,m=1}^{M}\begin{pmatrix} |[\mathbf{t}_{21}^{\uparrow\uparrow}]_{nm}|^2 & [\mathbf{t}_{21}^{\uparrow\uparrow}]_{nm}[\mathbf{t}_{21}^{\downarrow\uparrow}]_{nm}^{*} \\ [\mathbf{t}_{21}^{\uparrow\uparrow}]_{nm}^{*}[\mathbf{t}_{21}^{\downarrow\uparrow}]_{nm} & |[\mathbf{t}_{21}^{\uparrow\uparrow}]_{nm}|^2 \end{pmatrix}$$

$$= \frac{1}{2}(\mathbf{1} + \mathbf{P}_{\text{detect}}\cdot\hat{\boldsymbol{\sigma}}), \tag{19}$$

and experimentally measurable spin-polarization vector $\mathbf{P}_{\text{detect}}$. Figure 1(c) shows that in narrow wires, quantum coherence of transported spin quantified by $|\mathbf{P}_{\text{detect}}|$ remains close to 1 for $L \lesssim L_{\text{SO}}$. In wires of fixed length, suppression of spin decoherence in Fig. 1(d) is governed by the wire width W and the spin precession length L_{SO}, which are also invoked as characteristic length scales to explain recent experiments.[21] The preservation of spin coherence allows for spin-interference signatures to become visible in the shot noise in Fig. 1(a) as "Rabi oscillations" of the Fano factor between $F_{\sigma\to\sigma'} = 1/3$ and $F_{\sigma\to\sigma'} = 1$ along the L_{SO} scale.

V. DISCUSSION

The phenomenological model of Ref. 8, characterized by the spin-relaxation length L_s (which, in the bulk SO-coupled systems with weak disorder, is identical[15,18,24] to the spin precession length L_{SO}), finds $F_{\uparrow\to\uparrow\downarrow}(L \gg L_s) = 2/3$. This in contrast to our $F_{\uparrow\to\uparrow\downarrow}(L \gg L_{\text{SO}}) = 0.55$ governed by the parameters of microscopic Rashba Hamiltonian where further reduction of $F_{\uparrow\to\uparrow\downarrow}(L \gg L_s) < 0.55$ is induced by geometrical confinement effects increasing spin coherence.

As regards the spin-valve setups, the semiclassical (Boltzmann-Langevine) approach to spin-dependent shot noise employed in Ref. 7 predicts Fano factors $F_{\uparrow\to\uparrow}(L \gg L_s) = F_{\uparrow\to\downarrow}(L \gg L_s) = 1/3$ for arbitrary microscopic spin-relaxation processes within the normal region, while we find $F_{\uparrow\to\uparrow}(L \gg L_{\text{SO}}) = F_{\uparrow\to\downarrow}(L \gg L_{\text{SO}}) \simeq 0.7$ for a specific case of wide Rashba SO coupled wires. Furthermore, oscillatory behavior of the Fano factor versus L/L_{SO} exhibited in our Fig. 1, especially conspicuous when quantum coherence of (partially coherent $0 < |\mathbf{P}_{\text{detect}}| < 1$) spin is increased in narrow wires, cannot emerge from the approach of Ref. 7 where spin dynamics is characterized only by L_s (being much larger than mean free path with no restrictions imposed on its relation to the system size), rather than by the full spin-density matrix.

To elucidate the source of these apparent discrepancies, we provide in Fig. 3 detailed picture of auto- and cross-correlations between spin-resolved currents, as well as of spin-resolved conductances. It is obvious that oscillations of both $S_{22}^{\sigma\sigma'}$ and $G_{21}^{\sigma\sigma'}$ due to partially coherent spin precession, visible as long as $|\mathbf{P}_{\text{detect}}| > 0$, can be captured only through a ful quantum treatment of both spin dynamics and charge propagation (where spin memory between successive scattering events is taken into account[24]). The asymptotic value $F_{\uparrow\to\uparrow}(L \gg L_{\text{SO}})$, is determined by the shot noise $S_{22}^{\uparrow\uparrow}$ that is similar in both $L \ll L_{\text{SO}}$ and $L \gg L_{\text{SO}}$ limits, as well as by the value of charge current $I_2^{\uparrow} = G_{21}^{\uparrow\uparrow}V$ in the limit $L \gg L_{\text{SO}}$ where it becomes half of $I_2^{\uparrow}$ for vanishing SO coupling $L/L_{\text{SO}} \to 0$ [Figs. 3(b) and 3(e)]. This is due to the fact that at the exit of the normal region with $L/L_{\text{SO}} \gg 1$, charge current is unpolarized, so that one of its spin subsystems is completely reflected from the detecting spin-selective ("analyzer") electrode.

Figure 3(a) also reveals that unpolarized charge current flowing out of the Rashba SO-coupled region, after the injected fully spin-polarized current was completely dephased $|\mathbf{P}_{\text{detect}}| = 0$ along the Rashba wire, still displays nontrivial cross-correlations between spin-resolved currents encoded in $S_{22}^{\uparrow\downarrow} = S_{22}^{\downarrow\uparrow} \neq 0$. They reduce $S_{22}^{\uparrow\downarrow} = S_{22}^{\downarrow\uparrow} < 0$ our Fano factor $F_{\uparrow\to\uparrow\downarrow}(L \gg L_s) = 0.55$ below $F_{\uparrow\to\uparrow\downarrow}(L \gg L_s) = 2/3$ of Ref. 8 (which we recover approximately if we characterize the shot noise in the right lead only with $S_{22}^{\uparrow\uparrow} + S_{22}^{\downarrow\downarrow}$).

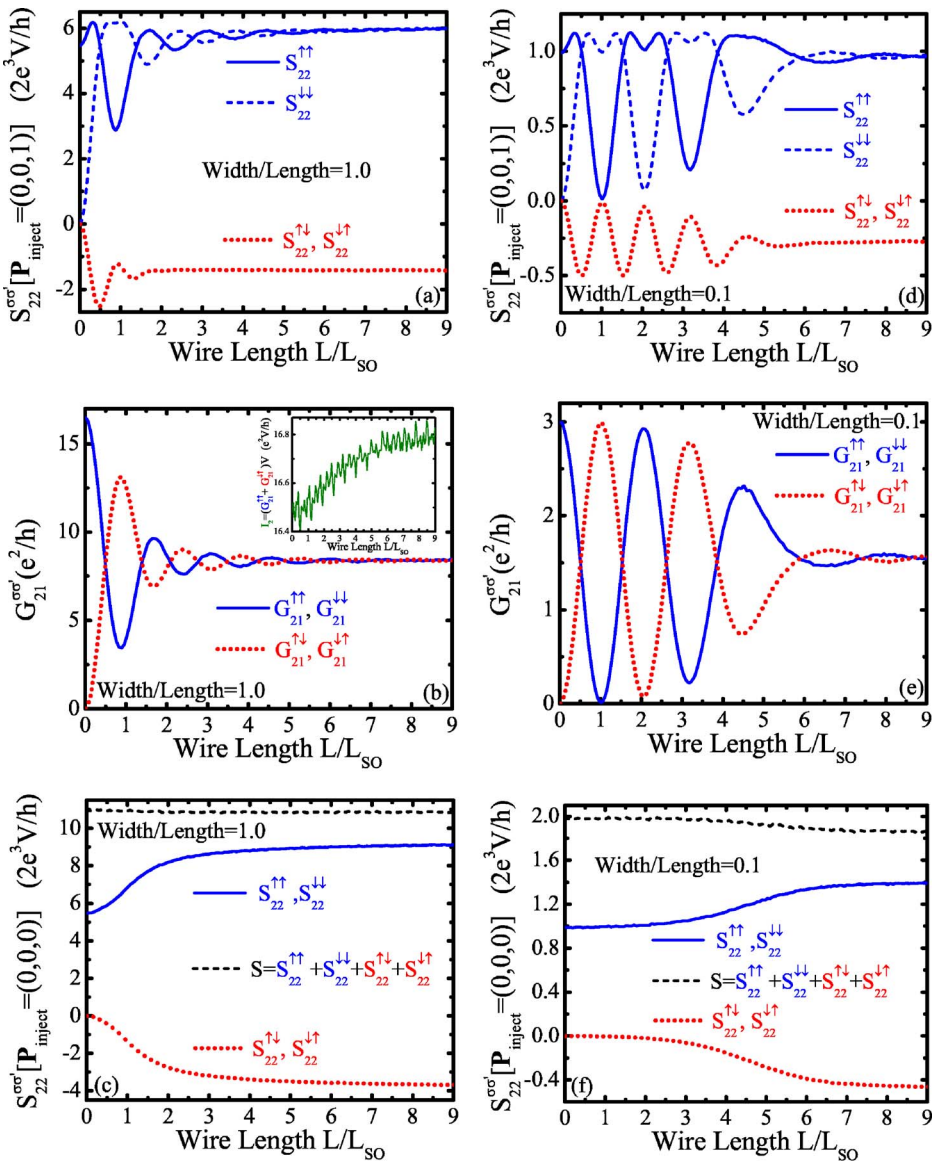

FIG. 3. (Color online) Zero-frequency spin-resolved shot-noise power $S_{22}^{\sigma\sigma'}$ [panels (a) and (d)] and spin-resolved conductances $G_{21}^{\sigma\sigma'}$ [panels (b) and (e)], which define different Fano factors in Fig. 1, for current detected in the right lead after the injection of spin-polarized (along the z axis) charge current from the left lead into the diffusive wire with the Rashba SO coupling of strength L/L_{SO}. The quantum wire is wide in panels (a)–(c) and narrow in panels (d)–(f). The inset in panel (b) shows weak antilocalization enhanced detected current in the right lead $I_2=I^{\uparrow}+I^{\downarrow}$ of ferromagnet/SO-coupled-wire/paramagnet setup. The spin-resolved shot noises for unpolarized current injection are shown in panels (e) and (f), whose sums give the limiting curves (for $|\mathbf{P}_{\mathrm{inject}}|=0$) in Fig. 2.

VI. CONCLUDING REMARKS

In conclusion, we have derived a scattering theory formula for the shot noise of charge and spin currents which takes as an input the degree of quantum coherence of injected spins $|\mathbf{P}_{\mathrm{inject}}|$, as well as the direction of the spin-polarization vector $\mathbf{P}_{\mathrm{inject}}$ with respect to relevant internal and external magnetic fields within the sample. The application of this formalism to two-terminal multichannel diffusive quantum wires with the Rashba SO coupling shows how decoherence and dephasing of spin dynamics are essential in observing the enhancement[7,8] of charge shot noise in spin-dependent transport. That is, in narrow wires, where loss of spin coherence is suppressed and $|\mathbf{P}_{\mathrm{detect}}|$ decays much slower [Figs. 1(c) and 1(d)] than in the bulk systems, increase of the Fano factor (above $F=1/3$ of spin-degenerate diffusive transport[5]) in the strong SO coupling regime ($L\gg L_{\mathrm{SO}}$ inducing fast spin dynamics within the sample) is reduced when compared to wide wires. This occurs despite the fact that *partially coherent* spin state continues to "flip" through partially coherent[17] spin precession $0<|\mathbf{P}_{\mathrm{detect}}|<1$. To obtain the Fano factor of charge currents comprised of partially coherent spins requires treating both charge propagation and spin dynamics quantum mechanically, as suggested by the spin-resolved shot noises and conductances in Fig. 3 (which cannot be reproduced by semiclassical approaches to spin-dependent shot noise where spin dynamics

is captured only through phenomenological spin-flip diffusion length[7]).

Finally, a remarkable one-to-one correspondence between the values of $F_{\uparrow\to\uparrow\downarrow}$ and the degree of quantum coherence $|\mathbf{P}_{\text{detect}}|$ predicted in Fig. 1(e) offers an exciting possibility of measuring the coherence properties of transported spin in a *purely charge transport experiment* on open SO-coupled systems, thereby offering an all-electrical alternative to usually employed optical tools to probe transport of spin coherence in semiconductors.[21]

ACKNOWLEDGMENT

This research was supported in part by the University of Delaware Research Foundation.

[1] Ya. M. Blanter and M. Büttiker, Phys. Rep. **336**, 1 (2000).
[2] H. Schomerus and P. Jacquod, J. Phys. A **38**, 10663 (2005).
[3] A. H. Steinbach, J. M. Martinis, and M. H. Devoret, Phys. Rev. Lett. **76**, 3806 (1996).
[4] E. Onac, F. Balestro, B. Trauzettel, C. F. J. Lodewijk, and L. P. Kouwenhoven, Phys. Rev. Lett. **96**, 026803 (2006).
[5] C. W. J. Beenakker and M. Büttiker, Phys. Rev. B **46**, 1889 (1992); K. E. Nagaev, Phys. Lett. A **169**, 103 (1992).
[6] Y. Tserkovnyak and A. Brataas, Phys. Rev. B **64**, 214402 (2001).
[7] E. G. Mishchenko, Phys. Rev. B **68**, 100409(R) (2003).
[8] A. Lamacraft, Phys. Rev. B **69**, 081301(R) (2004).
[9] K. E. Nagaev and L. I. Glazman, Phys. Rev. B **73**, 054423 (2006).
[10] W. Belzig and M. Zareyan, Phys. Rev. B **69**, 140407(R) (2004); M. Zareyan and W. Belzig, Europhys. Lett. **70**, 817 (2005).
[11] A. Cottet, W. Belzig, and C. Bruder, Phys. Rev. Lett. **92**, 206801 (2004).
[12] J. C. Egues, G. Burkard, and D. Loss, Phys. Rev. Lett. **89**, 176401 (2002); J. C. Egues, G. Burkard, D. S. Saraga, J. Schliemann, and D. Loss, Phys. Rev. B **72**, 235326 (2005).
[13] C. W. J. Beenakker, Phys. Rev. Lett. **81**, 1829 (1998).
[14] R. Winkler, *Spin-Orbit Coupling Effects in Two-Dimensional Electron and Hole Systems* (Springer, Berlin, 2003).
[15] I. Žutić, J. Fabian, and S. Das Sarma, Rev. Mod. Phys. **76**, 323 (2004).
[16] A. Ossipov, J. H. Bardarson, J. Tworzydło, M. Titov, and C. W. J. Beenakker, Europhys. Lett. **76**, 115 (2006).
[17] B. K. Nikolić and S. Souma, Phys. Rev. B **71**, 195328 (2005).
[18] A. G. Mal'shukov and K. A. Chao, Phys. Rev. B **61**, R2413 (2000); A. A. Kiselev and K. W. Kim, *ibid.* **61**, 13115 (2000).
[19] M. Büttiker, Phys. Rev. B **46**, 12485 (1992).
[20] L. E. Ballentine, *Quantum Mechanics: A Modern Development* (World Scientific, Singapore, 1998).
[21] A. W. Holleitner, V. Sih, R. C. Myers, A. C. Gossard, and D. D. Awschalom, Phys. Rev. Lett. **97**, 036805 (2006).
[22] O. Sauret and D. Feinberg, Phys. Rev. Lett. **92**, 106601 (2004).
[23] I. L. Aleiner and V. I. Fal'ko, Phys. Rev. Lett. **87**, 256801 (2001).
[24] T. P. Pareek and P. Bruno, Phys. Rev. B **65**, 241305(R) (2002).
[25] E. Joos, H. D. Zeh, C. Kiefer, D. Giulini, J. Kupsch, and I.-O. Stamatescu, *Decoherence and the Appearance of a Classical World in Quantum Theory*, 2nd ed. (Springer-Verlag, Heidelberg, 2003).
[26] S. Pramanik, S. Bandyopadhyay, and M. Cahay, IEEE Trans. Nanotechnol. **4**, 2 (2005).